

Effect of chain aggregation on the conductivity and ESR spectra of polyaniline

A. V. Kulikov,^{*} A. S. Komissarova, A. G. Ryabenko, L. S. Fokeeva, I. G. Shunina, and O. V. Belonogova

*Institute of Problems of Chemical Physics, Russian Academy of Sciences.
1 prosp. Akad. Semenova, 142432 Chernogolovka, Moscow Region, Russian Federation.
Fax: +7 (496) 515 3588. E-mail: kulav@icp.ac.ru*

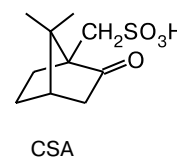
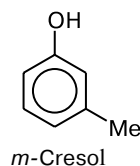
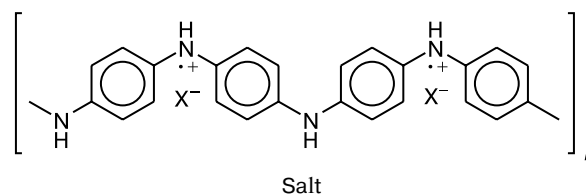
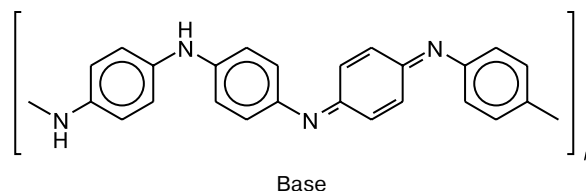
Solutions of polyaniline in *m*-cresol with and without camphorsulfonic acid (CSA), as well as films cast from these solutions were studied by ESR spectroscopy at 133–423 K and by optical spectroscopy in the range $\lambda = 350$ –1100 nm. An analysis of the optical and ESR spectra shows that in the solutions and films without CSA polyaniline is fully doped but the conductivity of these films is low ($\sim 10^{-8}$ S cm $^{-1}$; cf. 100 S cm $^{-1}$ for the films with CSA). Compared with the CSA-containing samples, the samples without CSA are characterized by broader ESR lines and higher contribution of the Curie spins to the magnetic susceptibility. These facts indicate a weak aggregation of polyaniline chains without CSA, which leads to low conductivity. A formula was proposed, which describes the temperature dependence of the polyaniline ESR linewidth and allows the interchain distance and the mobility of electrons moving along polymer chains to be determined. The conductivity of polyaniline films is affected by moderate heating (363–388 K) of the films and solutions from which the films were cast. It was found that the interchain distances correlate with the conductivity of the films and with the broadening of their ESR lines caused by the effect of O $_2$.

Key words: polyaniline, aggregation, conductivity, ESR spectroscopy.

Polyaniline films cast from polyaniline solutions in *m*-cresol containing camphorsulfonic acid (CSA) additives have been a subject of intensive research because they exhibit recordly high conductivities (see, e.g., Refs 1–7 and references cited therein). It is accepted that CSA favors transformation of polyaniline into a protonated conducting form and that *m*-cresol changes the conformation of the polyaniline molecules from a coil to extended chain. Extended chains are characterized by closer packing and the film conductivity increases due to fast inter-chain electron transfer.

Protonation of the basic form of polyaniline leads to the appearance of paramagnetic polarons.

Because of spatial periodicity of the "polaron" lattice the electron energy spectrum has a band structure. The upper band is partially filled, which is responsible for the high electronic conductivity and temperature-independent Pauli susceptibility. The conformation of polyaniline molecules can be affected by counterions X $^{-}$ and solvent molecules. Theoretical analysis⁸ showed that high solubility and extended conformation of the polyaniline molecules in solution in the *m*-cresol–CSA system is due to the formation of a specific complex polyaniline–*m*-cresol–CSA owing to combination of the stacking of phenyl groups, hydrogen bonding, and electrostatic interaction.



Conducting polymers including polyaniline are called quasi-1D metals, because their properties strongly depend on the interchain interaction. It was theoretically shown that the existence of true 1D metals is impossible, because any violation of periodicity leads to localization

of electrons (see, *e.g.*, Refs 9 and 10 and references cited therein). It is considered that the Pauli susceptibility of conducting polymers is due to the domains with close packing of chains (the so-called metal-like, quasi-3D high-conductivity domains) separated by quasi-1D low-conductivity domains and that the conductivity of conducting polymers is controlled by that of the quasi-1D domains. As temperature increases, the conductivity of conducting polymers increases, whereas the conductivity of normal metals decreases. An increase in the polyaniline conductivity with temperature is explained in terms of the variable range hopping model (see, *e.g.*, Refs 9 and 10), according to which thermally activated motion of electrons along the polymer chains is accompanied by inter-chain hopping at appropriate sites.

The effect of the inter-chain interaction on the conductivity, magnetic susceptibility, width of the ESR spectrum, and other characteristics of polyaniline films has been studied (see Refs 9–11 and references cited therein). Introduction of substituents into benzene rings leads to an increase in the interchain distances and in the proportion of localized spins, to a decrease in conductivity, to deviation of the shape of the ESR spectra in the wings from Lorentzian shape, and to some other effects.^{9–11} They are explained by enhancement of the 1D character of conductivity upon introduction of substituents.

m-Cresol itself can protonate (dope) polyaniline. In this connection it was interesting to compare the solutions of polyaniline in *m*-cresol without and with CSA additives as well as the films cast from these solutions. It was found that the conductivity of the films without CSA is much lower than that of the films with CSA additives. The results obtained in this work by 3-cm ESR spectroscopy suggest the absence of interchain interaction in the polyaniline samples containing no CSA. A relation was proposed, which describes the temperature dependence of the ESR linewidth and makes it possible to determine the interchain distances. It was found that differences between these distances are responsible for not only the difference in the film conductivities but also the distinctions in the oxygen effect and in the published 2-mm ESR spectra.

Experimental

Chemicals used in this work were aniline (Reakchim, Russia, "pure" grade), *m*-cresol (Aldrich, 98%), as well as CSA, HClO₄, and (NH₄)₂S₂O₈ (Reakchim, Russia, "chemically pure" grade).

Polyaniline was synthesized by oxidative polymerization at –20 °C. To 10 mL of 1 *M* aniline solution in MeCN containing 1 *M* HClO₄, 10 mL of a MeCN–water (3 : 4) mixture containing ammonium persulfate (1 mol L^{–1}) and 1 *M* HClO₄ was added dropwise over a period of 2 h. The emeraldine salt precipitate thus obtained was washed with alkali to obtain emeraldine base and dried at room temperature.

Films were prepared by deposition of polyaniline solutions on glass and lavsan supports followed by drying at room temperature. Lavsan is appropriate for both optical and ESR measurements because it produces no ESR signal and exhibits no absorbance in the 300–1100 nm region. Additionally, the films for ESR measurements can be rolled and placed in a glass tube (inner diameter 5 mm). Two types of films were prepared. The first type of films on lavsan supports were cast from a 4% (wt.) solution of polyaniline in *m*-cresol (without CSA) heated at 423 K for 1 h. These films were relatively thin (~1 μm thick). Their conductivity (~10^{–8} S cm^{–1}) was determined by the two-probe method and the film thickness was determined photometrically. To prepare the second type of films, a mixture of the basic form of polyaniline (12 mg) with CSA (18 mg) was thoroughly stirred in a porcelain mortar, *m*-cresol (0.6 mL) was added and the mixture was thoroughly stirred again. Paste (2 wt.%) thus obtained was deposited on the glass (for conductivity measurements) or lavsan (for optical and ESR measurements) support. These films were ~50 μm thick. The thickness of the films on glass supports were determined by a micrometer. The film conductivity (100 S cm^{–1}) was determined by the four-probe technique at a frequency of 1 kHz. Contacts were glued with Silver Point paste.

Digitized ESR spectra were recorded with an SE/X 2544 ESR spectrometer (Radiopan, Poznan, Poland) operating in the 3-cm band, equipped with a magnetometer, a frequency meter, and a temperature accessory. Solutions were placed in glass or polyethylene tubes (inner diameter ~1 mm) and films were placed in 5-mm glass tubes. When determining the second moments of the ESR spectra of polyaniline solutions in *m*-cresol, the spectra were recorded in the 20 mT range.

The ESR spectra of films were recorded in vacuum (~10^{–2} Torr) and in pure oxygen atmosphere (0.9 atm). A blank run involved removal of oxygen from a gel diluted with a large excess of *m*-cresol. To this end, the solutions were placed in thin-wall polyethylene tubes (inner diameter ~1 mm) with gas-permeable walls and the tubes were blown over with argon for 2–3 h at room temperature. The ESR linewidth remained unchanged. For a suspension of polyaniline in water, it took 30 min to remove oxygen. Thus, in *m*-cresol the effect of oxygen is insignificant and the ESR spectra of paste and solutions reported in this work were recorded in air.

The magnetic susceptibility was determined by comparing the second integrals of the ESR spectra of the polyaniline sample under study and a reference sample with the known spin concentration. In solution studies, a 1 mM solution of stable free nitroxyl radical in EtOH was used as the reference sample. The molar magnetic susceptibility of the nitroxyl radical at room temperature was assumed to be 1.5 · 10^{–3} (in dimensionless electromagnetic units, e.m.u.). The molar magnetic susceptibility of polyaniline solutions is reported per mole of two rings and the film susceptibilities are given in relative units because of problems in determining the film weight and considering the sample geometries.

In some cases the ESR lines were simulated by the sum of two Lorentzian lines with the same *g*-factors and different linewidths (*D*₁ and *D*₂) and intensities (*A*₁ and *A*₂) using the ORIGIN 6.0 program. The proportion of spins with the spectrum width *D*₁ was determined as $F_1 = A_1 D_1^2 / (A_1 D_1^2 + A_2 D_2^2)$. The temperature dependence of the linewidth was also simulated using the ORIGIN 6.0 program. The ESR spectra exhibiting

a hyperfine structure and the spectra with anisotropy of the g -factor were simulated using the Simfonia program.

As shown below, the width and shape of the ESR spectral lines in both polyaniline solutions and films can undergo irreversible changes on heating the sample; therefore, all temperature dependences were measured as follows. First, the temperature was lowered from 293 to 133 K and then raised to a maximum value (at most 423 K), and then decreased again to 293 K.

The optical spectra in the region $\lambda = 200\text{--}1100\text{ nm}$ were recorded with a Perkin–Elmer Lambda EZ 210 spectrophotometer.

Results and Discussion

Polyaniline doping with *m*-cresol. *m*-Cresol can dope, although slowly, polyaniline without CSA. This is not surprising because *m*-cresol is a weak acid characterized by a room-temperature acidity of 10, *i.e.*, $[A][H]/[AH] = 10^{-10}$. Hence, $[H] \approx 3 \cdot 10^{-5}\text{ mol L}^{-1}$.

A freshly prepared solution of the basic form of polyaniline in *m*-cresol has a blue color and exhibits a

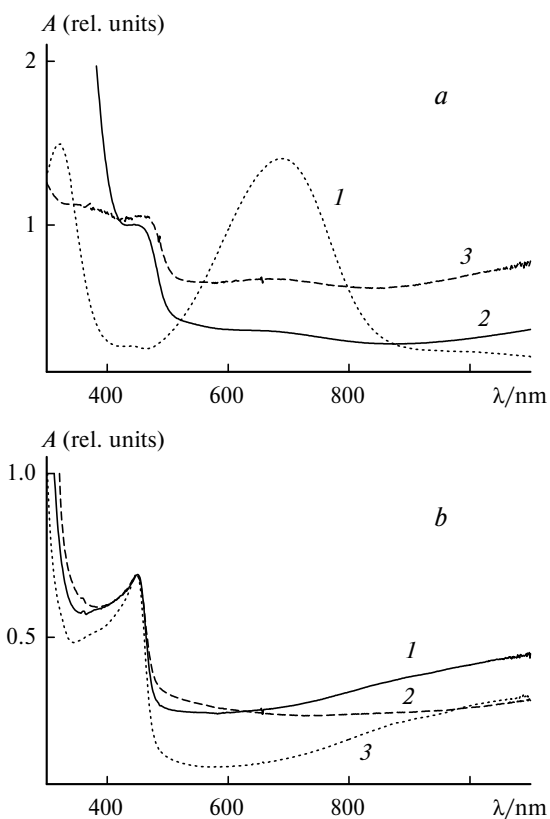


Fig. 1. Room-temperature absorption spectra of polyaniline solutions in *m*-cresol and of the films cast from these solutions: (a) 0.1% (wt.) solution of polyaniline in *m*-cresol 1 h after dissolution (1), solution after heating at 423 K for 1 h (2), and a film cast from the heated solution (3); (b) 2% polyaniline–CSA–*m*-cresol paste (1), film prepared from gel formed from the paste after 48 h (2), and gel after 30-fold dilution with *m*-cresol (3).

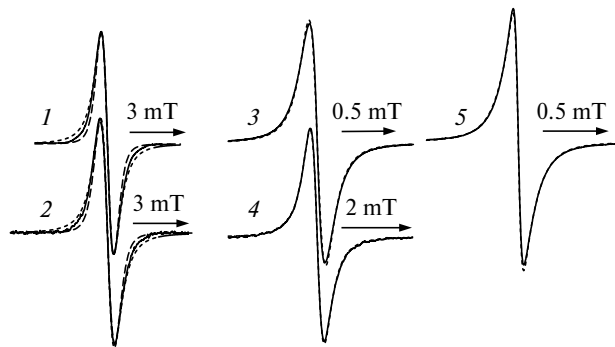


Fig. 2. Typical ESR spectra of polyaniline solutions and films and their simulations: 4% solution of polyaniline in *m*-cresol after heating (423 K, 1 h), 293 K (solid curve), Lorentzian (dash-and-dot) line, and 1D-line (dashed) (see text) (1); film cast from 4% solution of polyaniline in *m*-cresol after heating (423 K, 1 h), 293 K (solid curve), Lorentzian line (dash-and-dot), 1D-line (dashed) (1); freshly prepared 2% polyaniline–CSA–*m*-cresol paste, 133 K (solid curve), Lorentzian line (dash-and-dot) (3); film prepared from 2% polyaniline–CSA–*m*-cresol paste, 273 K (solid curve), Lorentzian line (dash-and-dot) (4); and 2% paste polyaniline–CSA–*m*-cresol after heating (90 °C, 10 min), 353 K (solid curve), sum of two Lorentzian lines 0.063 and 0.17 mT wide; the proportion of the narrow line (dash-and-dot) is 0.40 (5); the g -factors of all line are 2.0029 ± 0.0001 .

characteristic optical spectrum (Fig. 1, *a*, curve 1) and a very weak ESR signal of width $\sim 0.2\text{ mT}$. During a few days the solution gradually turns green, the band at 690 nm becomes less intense while the intensity of the band at 440 nm increases and the intensity of the ESR signal of width $\sim 1\text{ mT}$ also increases. The doping is accelerated at 423 K (heating at this temperature for 1 h is sufficient to obtain unchangeable patterns of the optical and ESR spectra). The optical spectrum of the solution after heating is similar to the spectrum of the polyaniline solution in *m*-cresol with CSA additives (see Fig. 1, *a*, curve 2, and Fig. 1, *b*, curve 1). Once heated, this solution exhibits an intense ESR signal (Fig. 2, curve 1).

The optical and ESR spectra of the heated solution are independent of concentration in the range 0.05–4% (wt.) and exhibit no changes over a period of a few months.

The optical and ESR spectra of the films cast from this solution are similar to the solution spectra (see Fig. 1, *a*, curves 2 and 3, and Fig. 2, curves 1 and 2).

Gel formation in the presence of CSA. A 2% polyaniline–CSA–*m*-cresol paste prepared as reported above (see Experimental) is transformed into gel over a period of a few hours at room temperature. This indicates the formation of a 3D-network owing to aggregation of polyaniline chains. The optical spectra of the gel and of the film prepared from it are similar to the spectra of the heated solution of polyaniline in *m*-cresol without CSA

and of the films cast from solution (see Fig. 1). The ESR spectra of the solutions and films with CSA additives are characterized by narrower ESR lines compared to the spectra of the samples without CSA (see Fig. 2, curves 3–5). The linewidth decreases due to exchange interactions between aggregated chains (more detailed consideration is given below).

A 30-fold dilution of the gel with *m*-cresol is followed by the broadening of the ESR line from 0.12 to 0.23 mT. However, the addition of CSA to the dilute solution causes the ESR line to narrow to its initial width. The optical spectrum of the dilute gel is almost identical to that of the initial gel (*cf.* curves 1 and 3 in Fig. 1, *b*). The effect of dilution on the ESR linewidth can be explained by dissociation of the polyaniline–CSA complex on dilution followed by an increase in the interchain distances.

Thus, the data obtained in this work show that CSA favors aggregation of polyaniline chains.

Analysis of ESR lineshape. Analysis of the ESR lineshape also indicates strengthening of the interchain interaction in the presence of CSA (Figs 2 and 3). The shape of the ESR spectra of the solution of polyaniline in *m*-cresol and of the film cast from this solution noticeably differs from Lorentzian shape in the wings, whereas the ESR spectra recorded in the presence of CSA almost completely match the Lorentzian shape (see Fig. 2, curves 1–4). This is more pronounced in the anamorphoses of the ESR lines plotted in the $A_0/A(H) - [(H - H_0)/\Delta H]^2$ coordinates, where $A(H)$ is the first derivative of the ESR spectrum, A_0 is the peak-to-peak line amplitude, H is the magnetic field strength,

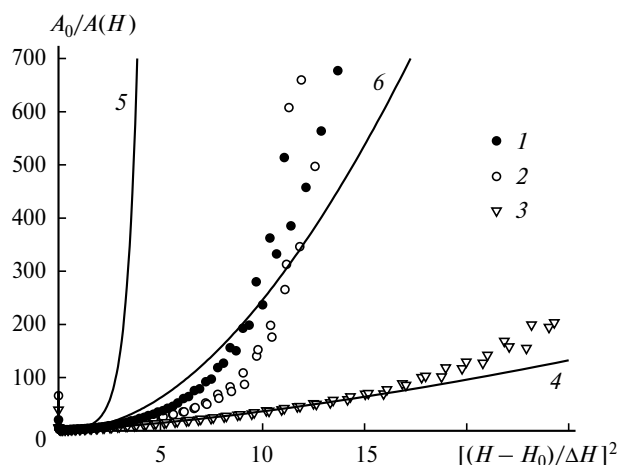


Fig. 3. Anamorphoses of the ESR line of polyaniline solutions: 4% solution of polyaniline in *m*-cresol after heating (423 K, 1 h) at 133 and 293 K, respectively (1 and 2); freshly prepared 2% polyaniline–CSA–*m*-cresol paste at 293 K (3). Shown are the anamorphoses for both wings of each spectrum. Solid lines are the anamorphoses of the Lorentzian (4) and Gaussian line (5), and line for the 1D case (1-D, see text, 6).

and ΔH is the peak-to-peak linewidth (see Fig. 3). Note that usually the anamorphosis is plotted for the integral of the spectral line (see, *e.g.*, Refs 9 and 10) and in this case A_0 is the line amplitude at $H = H_0$ and ΔH is the half-width at half-height. Then, the anamorphosis of a Lorentzian line is a straight line. In the coordinates we used the anamorphosis of the Lorentzian line is somewhat nonlinear; however, in these coordinates it is possible to analyze the first derivative recorded by the ESR spectrometer without pre-integration of the spectral line, which introduces some errors.

Qualitative consideration of the spin-motion induced narrowing of magnetic resonance lines based on calculations of the moments of spectral lines showed¹² that the narrowed lines always have a Lorentzian shape at the center. However, in the wings the line amplitudes decrease faster compared to the Lorentzian line and the greater the degree of line narrowing, the better the description of the line by the Lorentzian curve.

For polyaniline, deviations of the ESR lineshape in the wings from the Lorentzian contour are usually explained^{9,10} (see also references cited in these studies) by the 1D character of spin motions. Assuming that the main mechanism of ESR line broadening in conducting polymers involves the magnetic dipole-dipole interactions between electrons within the same chain, the theory predicts that in the case of isolated chains the ESR line should be described by the Fourier image of the function $\exp(-at^{3/2})$. The first derivative of this 1-D line is shown in Fig. 2 (curves 1 and 2) and its anamorphosis is presented in Fig. 3. As the exchange interaction between polyaniline chains strengthens, the lineshape should be more and more similar to Lorentzian.¹⁰

The 1-D line incorrectly describes the wings of the ESR line (see Figs 2 and 3); therefore, it is unlikely that the dipole-dipole interactions between electrons within the same chain give the major contribution to the linewidth.

Thus, analysis of the ESR lineshape shows that without CSA the interchain interaction is weak both in solution and in the film cast from this solution, whereas in the presence of CSA the polymer chains aggregate and the exchange interaction between electrons of neighboring chains causes narrowing of the ESR line.

The ESR line of paste after heating (363 K, 10 min) fits well by the sum of two lines (see Fig. 2, curve 5) with different widths, which can be explained by the presence in the sample of two types of domains characterized by different degree of chain packing.

Temperature dependences of magnetic susceptibility.

The temperature dependences of the linewidths and magnetic susceptibilities of solutions and films cast both in the presence of and without CSA additives are shown in Figs 4–7. From the temperature dependence of the

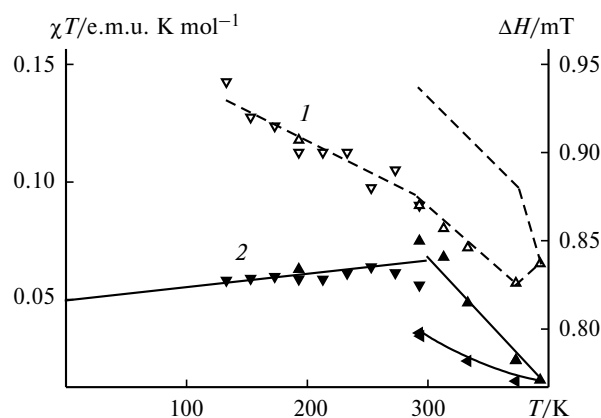


Fig. 4. Temperature dependence of the ESR linewidth (1) and χT parameter (2) for 4% solution of polyaniline in *m*-cresol after heating (423 K, 1 h). Triangles directed down denote the data obtained on lowering the temperature from 293 K, triangles directed upward denote the data obtained on subsequent heating to the maximum temperature, and triangles directed to the left denote the data obtained on lowering the temperature from the maximum value.

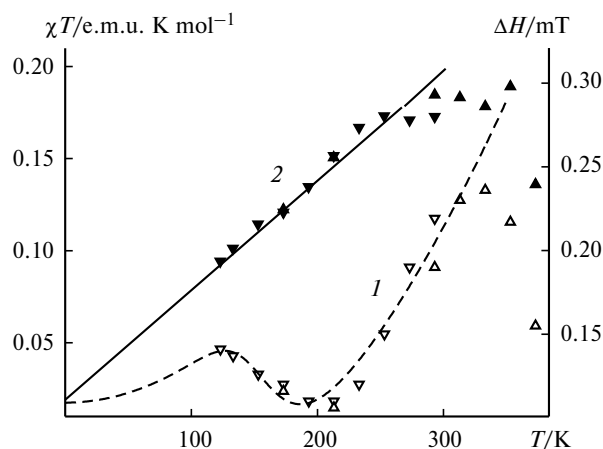


Fig. 5. Temperature dependence of the ESR linewidth (1) and χT parameter (2) for freshly prepared 2% polyaniline—CSA—*m*-cresol paste. For notations, see Caption to Fig. 4. Dashed line denotes the results of calculations using expression (6) with the parameters listed in Table 2.

χT parameter it is possible to determine the Pauli susceptibility χ_P and the number, n_C , of localized spins:

$$\chi T = \chi_P T + C, \quad (1)$$

where C is the Curie constant, which is independent of temperature and proportional to the number, n_C , of localized spins. According to expression (1), the χT parameter should be a linear function of temperature and the χ_P and n_C values are determined from the slope of the straight line and the intercept at $T = 0$, respectively. It should be recalled that, since often the temperature dependences are irreversible, they were obtained by initially lowering

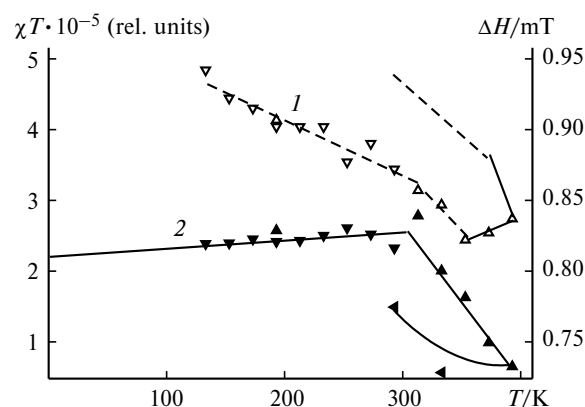


Fig. 6. Temperature dependence of the ESR linewidth (1) and χT parameter (2) for evacuated film cast from the 4% polyaniline solution in *m*-cresol after heating (423 K, 1 h). For notations, see Caption to Fig. 4.

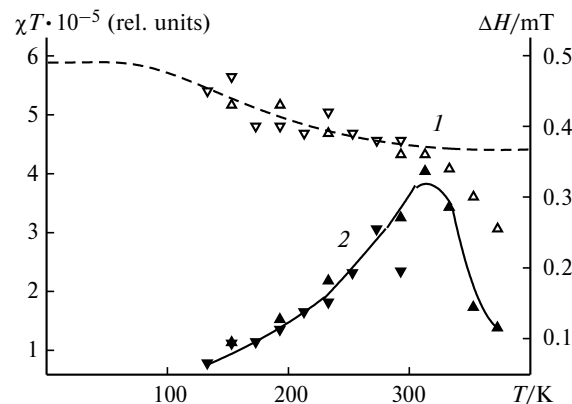


Fig. 7. Temperature dependence of the ESR linewidth (1) and χT parameter (2) for evacuated film from freshly prepared 2% paste polyaniline—CSA—*m*-cresol. Dashed line denotes the results of calculations using expression (6) with the parameters listed in Table 2.

the temperature from room temperature, then raising it to ~400 K and then by lowering again. In most cases relation (1) holds for the temperatures below room temperature and the χT parameter always decreases as the temperature is raised above ambient temperature. In some cases (see below) raising the temperature above room temperature leads to asymmetrization of the ESR line, which indicates the formation of a skin layer acting as a shield for a part of spins. However, the main reason for the decrease in χT with an increase in temperature above ambient temperature consists in transition of a part of the paramagnetic form of polyaniline into the diamagnetic form due to dedoping or formation of diamagnetic bipolarons.

CSA-Containing films exhibit a nonlinear temperature dependence of χT at low temperatures (see Fig. 7), which is usually explained by the spin-spin exchange interaction.^{13,14}

Table 1. Pauli magnetic susceptibility (χ_p) and the amount of Curie spins (n_C) for polyaniline solutions

Sample	$\chi_p^* \cdot 10^6$ /e.m.u.	n_C^*
Solution of polyaniline (4%) in <i>m</i> -cresol after heating (423 K, 1 h)	35–55	0.11–0.12
Freshly prepared 2% poly- aniline—CSA— <i>m</i> -cresol paste	60	0.005
Paste after heating (363 K, 10 min)	28	0.0035

* Per mole of two rings.

The χ_p and n_C values for solutions, obtained at temperatures below room temperature, are listed in Table 1. For films, these parameters were not measured owing to difficulties with the determination of the film weights and the residual amount of *m*-cresol in the films. The data in Table 1 show that the solution of polyaniline in *m*-cresol without CSA is characterized by lower χ_p value and much larger parameter n_C compared to freshly prepared polyaniline—CSA—*m*-cresol paste. The conclusion that the contribution of the Curie susceptibility increases in the absence of CSA can also be drawn for films (*cf.* Figs 6 and 7). This is explained by the fact that in true 1D conductors any violations of the periodicity by chain defects lead to spin localization (see Refs 9 and 10 and references cited therein). If exchange interaction between chains is rather strong, the energy band structure is retained in the presence of chain defects.

Thus, analysis of the temperature dependence of the magnetic susceptibility suggests that without CSA the interchain interaction is weak both in solution and in the film; CSA acts as a "glue" for polyaniline chains in solution.

Temperature dependences of ESR linewidths. The temperature dependences of the peak-to-peak ESR linewidths of the solutions and films cast both in the presence and in the absence of CSA are shown in Figs 4–7. The temperature dependences for the solution and films without CSA are similar (*cf.* Figs 4 and 6). Raising the temperature from 133 to ~370 K is accompanied by line narrowing but further heating leads to irreversible line broadening. The line narrowing on heating to 370 K can be explained by acceleration of the motion of electrons along polymer chains (detailed analysis is given below). At ~300 K, the temperature dependences of the linewidths for both solution and films exhibit clearly seen kinks. Probably, this can be explained by the melting of *m*-cresol at 281–283 K and, as a consequence, by intensification of the molecular motions of polymer chains. Line broadening on heating above 370 K can be explained similarly to the decrease in the χT parameter by the dedoping of polyaniline.

A decrease in the degree of doping violates periodicity of the polymer chain and hampers the motion of electrons along the polymer chain.

The temperature dependence of the ESR linewidth for freshly prepared polyaniline—CSA—*m*-cresol paste (see Fig. 5) has a complex shape. As the temperature increases from 133 to 190 K, the line becomes narrower due to more intense motion of electrons along the polymer chain. Line broadening at temperatures above 190 K is usually explained (see, *e.g.*, Refs 10 and 15) by the spin-phonon interaction induced spin relaxation by the Elliott mechanism (also called the direct mechanism). This mechanism predicts a linear increase in the linewidth with an increase in temperature. As will be shown below, another mechanism (Raman mechanism) is more probable.

In the text below we propose a relation for the description of the temperature dependence of the ESR linewidth. Other expressions for calculating the ESR linewidth were also put forward.^{10,16,17} The distinctive features of our approach are the ESR line narrowing due to simultaneous motion of electrons along the polymer chain and inter-chain exchange interaction and the description of the spin-phonon interaction induced spin relaxation by the Raman mechanism instead of the direct one.

Relation for the description of the temperature dependence of the ESR linewidth. According to quantitative theory of spin relaxation, the following expressions for the spin-lattice and spin-spin relaxation times T_1 and T_2 , respectively (see, *e.g.*, Ref. 18), are valid in the presence of spin motions:

$$1/T_1 = 1/T_{10} + \gamma^2 (\overline{H_x^2} + \overline{H_y^2}) \frac{\tau}{1 + \omega^2 \tau^2}, \quad (2)$$

$$1/T_2 = 1/T_{20} + \gamma^2 \left(\overline{H_z^2} \tau + \overline{H_y^2} \frac{\tau}{1 + \omega^2 \tau^2} \right), \quad (3)$$

where $\gamma = 1.77 \cdot 10^8 \text{ mT}^{-1} \text{ s}^{-1}$ is the gyromagnetic ratio for an electron, H_i is the fluctuating magnetic field strength, ω is the frequency at which the ESR spectra are recorded (in rad s^{-1} ; in our case, $\omega \sim 6 \cdot 10^{10} \text{ s}^{-1}$), and τ is the correlation time of the fluctuating fields. These relations hold at

$$\gamma^2 (\sum H_i^2) \tau^2 \ll 1. \quad (4)$$

In contrast to the known expressions,^{16–18} relations (2) and (3) include two terms, $1/T_{10}$ and $1/T_{20}$, which allow for other spin relaxation processes. The quantitative theory predicts the Lorentzian lineshape. According to the qualitative theory,¹² this is not the case in the wings of the line, namely, the line amplitude in the wings should always decrease faster than the wings of the Lorentzian line. It is this case that is observed for polyaniline solutions and films containing no CSA (see Figs 2 and 3).

Suppose that the relaxation rates $1/T_{10}$ and $1/T_{20}$ are governed by the spin-phonon interactions and the following relation is valid:

$$1/T_{10} = 1/T_{20} = AT^n, \quad (5)$$

where T is temperature. Earlier, for two synthetic metals, polyaniline and popypyrrole, it was assumed that $1/T_{20} \sim T$ (see, e.g., Refs 10 and 15), i.e., $n = 1$, which corresponds to the direct mechanism of spin relaxation. However, this process is efficient only at temperatures below 10 K while the Raman mechanism with $n = 2$ predominates at higher temperatures.^{12,19} Additionally, the efficiency of the direct mechanism is proportional to ω^2 while that of the Raman mechanism is independent of ω ;^{12,19} therefore, the ESR linewidth should considerably increase in high-field measurements. However, on going from the 3-cm to the 2-mm band (a 225-fold increase in ω^2), the linewidth increases^{20,21} by 2 or 3 times only, which can be explained by increasing the role of anisotropy of the g -factor (see below). On the experimental data were analyzed assuming $n = 2$.

The equality $1/T_{10} = 1/T_{20}$ was confirmed experimentally. From relations (2), (3), and (5) it follows that if the linewidth proportional to $1/T_2$ increases with temperature, the terms $1/T_{10}$ and $1/T_{20}$ make the major contributions to $1/T_1$ and $1/T_2$, and $T_1 \approx T_2$. Otherwise, the second terms in relationships (2) and (3) predominate, and at $\omega\tau > 1$ one has $T_1 > T_2$. This holds for polyaniline²² and popypyrrole.^{16,17}

Assuming that $\bar{H}_x^2 = \bar{H}_y^2 = \bar{H}_z^2$ and taking into account that the peak-to-peak linewidth is $\Delta H = 2/(\sqrt{3}\gamma T_2)$, at $n = 2$ from relations (3) and (5) it follows that

$$\Delta H = AT^2 + \frac{2\gamma\bar{H}_z^2}{\sqrt{3}} \left(\tau + \frac{\tau}{1 + \omega^2\tau^2} \right). \quad (6)$$

Suppose that in the case of line narrowing due to the spin motions and static exchange interaction simultaneously a relation similar to the expression for the rate constant for two competing reactions holds:

$$1/\tau = 1/\tau_m + J, \quad (7)$$

where the exchange interaction constant J is expressed in rad s^{-1} and is temperature independent and the temperature dependence of the spin-motion correlation time τ_m is given by a relation for thermally activated motions

$$\tau_m = \tau_\infty \exp[E_a/(kT)], \quad (8)$$

where E_a is the activation energy, k is the Boltzmann constant ($8.3 \text{ J K}^{-1} \text{ mol}^{-1}$), and τ_∞ is the correlation time at infinitely high temperature.

At $J \gg 1/\tau_m$, the second term in expression (6) is proportional to \bar{H}_z^2/J ; the theories of exchange line narrowing lead to the same expressions (see, e.g., Ref. 12).

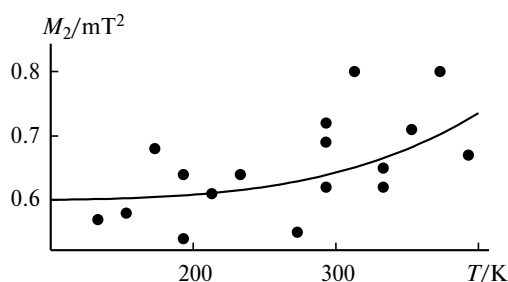


Fig. 8. Temperature dependence of the second moment of the ESR line (circles) of the 4% solution of polyaniline in *m*-cresol after heating (423 K, 1 h). Solid line — denotes the results of calculations using expression (9) with $\bar{H}_z^2 = 0.60 \text{ mT}^2$ and $A = 2.3 \cdot 10^{-6} \text{ mT K}^{-1}$.

The term \bar{H}_z^2 appeared in expression (6) can be determined from the temperature dependence of the second moment of the ESR line. According to the qualitative theory of line narrowing due to spin motions,¹² the contribution of local fields to the second moment \bar{H}_z^2 is temperature independent and the temperature dependence of the second moment should be described as follows

$$M_2 = A^2T^4 + \bar{H}_z^2. \quad (9)$$

The temperature dependence of the second moment line ESR of polyaniline solution in *m*-cresol is shown in Fig. 8. As can be seen, for this sample one has $\bar{H}_z^2 \approx 0.6 \text{ mT}^2$.

What is the nature of the local fields? They can be due to the hyperfine interaction between electrons and atomic nuclei of H and N, the magnetic dipole-dipole interactions between electron spins, and to anisotropy of the g -factor. As will be shown below, anisotropy of the g -factor makes a small contribution to the \bar{H}_z^2 quantity in the 3-cm ESR band. The measured HFI constants for $[\text{X}-\text{C}_6\text{H}_4-\text{NH}-\text{C}_6\text{H}_4-\text{Y}]^{+\cdot}$ fragments are as follows:²¹ $a_{\text{H}}(1 \text{ H}) = 0.79 \text{ mT}$, $a_{\text{H}}(4 \text{ H}) = 0.16 \text{ mT}$, $a_{\text{H}}(4 \text{ H}) = 0.086 \text{ mT}$, and $a_{\text{N}}(1 \text{ N}) = 0.79 \text{ mT}$. The second moment of the ESR spectrum simulated using these values is 0.60 mT^2 , which is similar to the experimentally determined second moment of the ESR spectrum of the polyaniline solution in *m*-cresol. Thus, the major contribution to \bar{H}_z^2 comes from the HFI.

The experimental temperature dependence of the linewidth was approximated by relation (6) with $\omega = 6 \cdot 10^{10} \text{ rad s}^{-1}$ and $\bar{H}_z^2 = 0.6 \text{ mT}^2$ and the temperature dependence of τ was described by expressions (7) and (8). The results of approximation for different samples are presented in Table 2, which also lists the interchain distances R calculated using the J values and the expression²³

$$J = 10^{17} \exp(-R/0.035), \quad (10)$$

where the J values are given in rad s^{-1} and R is given in nm. This expression was derived in the course of analy-

Table 2. Parameters J , R , t_{∞} , E_a , and A of the polyaniline solutions, powders, and films obtained in the approximation of the temperature dependence of the ESR linewidth using relation (6)^a

Sample	$J/\text{rad s}^{-1}$	R/nm	t_{∞}/s	$E_a/\text{kJ mol}^{-1}$	$A/\text{mT K}^{-2}$	Reference
Freshly prepared 2% paste poly-aniline—CSA— <i>m</i> -cresol	$1.1 \cdot 10^9$	0.64	$8 \cdot 10^{-14}$	13	$2.3 \cdot 10^{-6}$	This work
Film prepared from fresh 2% polyaniline—CSA— <i>m</i> -cresol paste ^c	$2.5 \cdot 10^8$	0.69	$2.6 \cdot 10^{-9}$	3.0	$4 \cdot 10^{-7}^b$	This work
Powder PAN1 ^c	$2.5 \cdot 10^9$	0.61	$5.6 \cdot 10^{-13}$	20	$4.2 \cdot 10^{-7}$	24
Powder PAN2 ^c	$6.4 \cdot 10^8$	0.66	$1.6 \cdot 10^{-10}$	2.9	$5.3 \cdot 10^{-7}$	24
Film PAN-ES ^c	$4.3 \cdot 10^9$	0.59	$2.0 \cdot 10^{-10}$	1.8	$1 \cdot 10^{-7}$	10
Freshly prepared 2% poly-aniline—CSA— <i>m</i> -cresol paste after heating (363 K, 15 min)	$1.3 \cdot 10^9$	0.64	$3.4 \cdot 10^{-12}$	6.0	$1.7 \cdot 10^{-7}$	This work

^a Approximated with $\bar{H}_z^2 = 0.6 \text{ mT}$ and $\omega = 6 \cdot 10^{10} \text{ rad s}^{-1}$.^b Approximated with $A = 4 \cdot 10^{-7} \text{ mT} \cdot \text{K}^{-2}$.^c Samples were evacuated.

sis of the experimental data for mainly biological systems in the 0.3—1.5 nm range.

Unambiguous determination of all parameters in relation (6) requires the temperature dependence study over a wide temperature range from room temperature to helium temperatures. Prior to comparing the values we have measured over a relatively narrow temperature range, we will analyze the available data^{10,24} on the linewidths, obtained in the range from room temperature to helium temperatures.

Analysis of published temperature dependences of the ESR linewidth. Figure 9 shows three main types of temperature dependences of the ESR linewidth for polyaniline. Namely, the linewidth decreases (*a*), increases (*b*), and passes through a minimum (*c*) as the temperature increases. Here, the solid lines represent the results of approximation using expression (6) with the parameters listed in Table 2. As can be seen, relation (6) provides quite a correct approximation of the experimental dependence with the parameters similar to those obtained by other methods. For instance, according to X-ray diffraction data,²⁵ the minimum distances between polyaniline chains lie in the range 0.57—0.70 nm. NMR studies of CSA-doped polyaniline films gave $\tau_{\infty} = 3 \cdot 10^{-14} \text{ s}$ and $E_a = 16 \text{ kJ mol}^{-1}$.

Analysis of the temperature dependences of ESR linewidth. Variability of polyaniline solutions and films. The temperature dependences of the ESR linewidths for solutions and films containing no CSA (see Figs 4 and 6) were not approximated because of small line narrowing, *i.e.*, condition (4) is not met and relation (6) is inapplicable.

The approximations plotted for CSA-containing polyaniline solution and film using expression (6) with the parameters listed in Table 2 are shown in Figs 5 and 7. For the CSA-containing films (see Fig. 7) the experimental

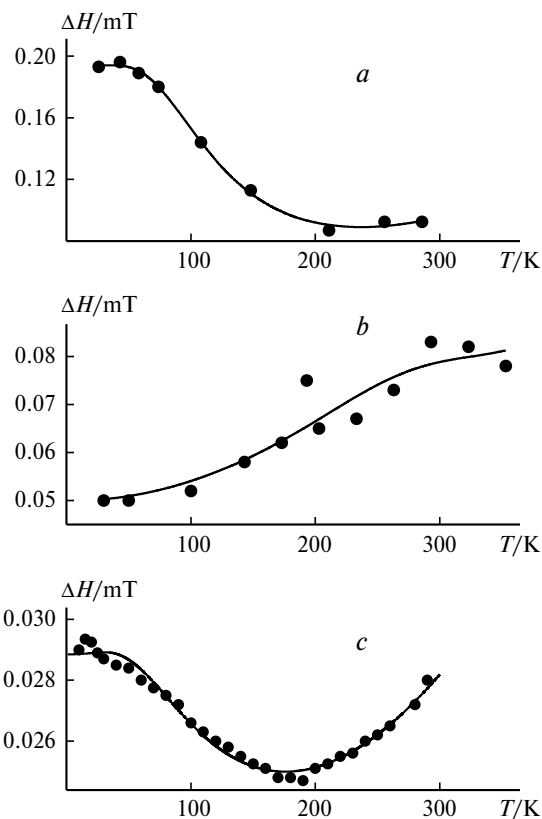


Fig. 9. Temperature dependence of the ESR linewidth (circles) of evacuated polyaniline powders and films (published data): PAN2 powder (*a*),²⁴ PAN1 powder (*b*),²⁴ and PAN—ES film (*c*).¹⁰ Solid line denotes the results of approximation using expression (6) with the parameters listed in Table 2.

temperature dependence of the linewidth is such that the parameter A cannot be determined unambiguously; its value was set to be $4 \cdot 10^{-7} \text{ mT K}^{-1}$ (typical parameter in Table 2). As can be seen, the approximations exhibit fea-

tures at lower temperatures, at which experiments were carried out, *i.e.*, measurements at low temperatures would be informative.

At temperatures above 333 K, the ESR linewidth and the magnetic susceptibility of freshly prepared polyaniline—CSA—*m*-cresol paste decrease (see Fig. 5) and the lineshape becomes asymmetric. The asymmetry parameter A/B (ratio of the deviations of the low- and high-field extrema from the baseline) increases to 2.0. These changes are irreversible, that is, after cooling to 293 K the linewidth is 0.11 mT and the A/B ratio is 2.0. Visual examination of the sample showed that heating above 333 K lead to coagulation of polyaniline into a bundle surrounded with a transparent substance (*m*-cresol). A decrease in the cavity Q-factor and an increase in the A/B ratio indicate a high conductivity of the bundle in the UHF-band. According to Dyson's theory,^{27,28} asymmetry of a spectral line is determined by the ratio of the sample size to the skin-layer thickness, which decreases as the conductivity increases. The skin layer acts as a shield for the interior of the sample; therefore, the magnetic susceptibility decreases. The line becomes symmetrical if the skin-layer thickness exceeds the sample size (*i.e.*, for small samples or for samples with low conductivity). After stirring of the coagulated sample the A/B ratio again becomes equal to unity, the second integral of the ESR line increases by a factor of ~ 1.5 while the ESR line remains narrow (0.12 mT). Thus, although stirring leads to a decrease in the size of polyaniline aggregates, the interchain interaction on the molecular level is retained.

The ESR linewidth of the film prepared from 2% polyaniline—CSA—*m*-cresol paste reversibly decreases as the temperature changes in the range 133–313 K (see Fig. 7). On heating above 313 K, the line becomes asymmetrical. Asymmetry is also retained on cooling to 293 K after heating at 373 K ($A/B = 1.36$, $\Delta H = 0.28$ mT). Asymmetry of the line indicates the possibility for changes in the chain packing to occur in the films even at high temperatures, thus leading to an increase in the conductivity at a frequency of 9 GHz.

The temperature dependences of the ESR linewidths for the paste heated at 363 K for 15 min are shown in Fig. 10. Noteworthy is the ESR line narrowing at 293 K after heating of the paste compared to the initial linewidth. As the temperature decreases below 293 K, the linewidth decreases even more to 0.07 mT. Similarly to the freshly prepared unheated paste, raising the temperature above 333 K causes irreversible changes in the ESR spectra due to formation of the bundle of polyaniline (the A/B ratio increases to a value of 2.19 at 293 K). After heating the susceptibility appreciably decreases (these data are not shown). The dash-and-dot line denotes the approximation of the linewidth using expression (6) with the parameters listed in Table 2.

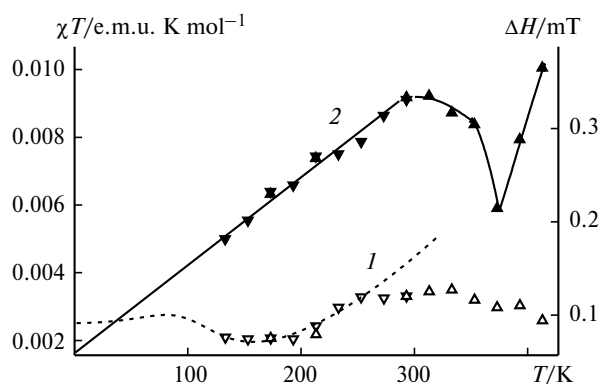


Fig. 10. Temperature dependence of the ESR linewidth (I) and χT parameter (2) for 2% solution of polyaniline in *m*-cresol with CSA additives heated to 363 K for 15 min. Dashed line denotes the results of calculations using expression (6) with the parameters with the parameters listed in Table 2. For notations, see Caption to Fig. 4.

Keeping the sample at room temperature for a few hours also led to the narrowing of the ESR line of this paste to 0.12 mT, as after keeping at 363 K for 15 min. As mentioned above, this leads to gel formation.

Film conductivities and interchain interaction. The conductivity of a polyaniline film cast from solution in *m*-cresol (without CSA) is very low (Table 3). From the aforesaid it follows that this can be explained by weak interaction between polyaniline chains in this film.

As mentioned above, heating of the films containing CSA at 388 K for 15 min is followed by the appearance of line asymmetry indicating an increase in the conductivity

Table 3. Conductivities (σ), ESR linewidths in vacuum (ΔH), broadening of the ESR lines in oxygen atmosphere at a pressure of 0.9 atm ($\Delta\Delta H$), and the asymmetry parameters of the ESR lines (A/B) for different polyaniline films*

Film	σ /S cm ⁻¹	ΔH $\Delta\Delta H$ mT		A/B
Film cast from 4% solution of polyaniline in <i>m</i> -cresol, heated at 423 K for 1 h	10^{-8}	0.87	<0.01	1.03
Film prepared from fresh 2% polyaniline—CSA— <i>m</i> -cresol paste	100	0.37	0.4	1.04
Film prepared from fresh 2% polyaniline—CSA— <i>m</i> -cresol paste after heating of the film at 388 K for 15 min	100	0.28	0.27	1.36
Film prepared from gel formed from 2% polyaniline—CSA— <i>m</i> -cresol paste after 48 h	150	0.12	0.1	1.26

* All quantities were measured at room temperature.

at the operating frequency of the radiospectrometer (~ 9 GHz). However, the conductivity measurements of the films heated at 388 K for 15 min showed no changes in the conductivity within the limits of experimental error (10%) (see Table 3). These data are in agreement with the published results,²⁹ according to which heating of polyaniline—CSA films at 408 K for 30 min leads to an insignificant (by $\sim 5\%$) decrease in the room-temperature conductivity and to a similar increase in the conductivity at low temperatures, although the degree of crystallinity and the optical spectra after annealing are changed.

Note that the conductivity of the film prepared from the gel is higher than the conductivity of the films fabricated from freshly prepared polyaniline—CSA—*m*-cresol paste. This can be explained by the fact that, judging from the ESR linewidth, the film prepared from gel is characterized by a shorter interchain distance than the film prepared from the fresh mixture.

Strictly speaking, it seems not to be too unlikely that in some cases the film conductivities and the ESR linewidths do not correlate. Indeed, according to widely accepted concepts, the conductivity is governed by the amorphous quasi-1D domains while the linewidth is determined by the metallic quasi-3D domains with close chain packing. Using ESR spectroscopy, it is possible to detect domains with different degrees of chain packing. For instance, the ESR spectrum of the gel fits well by the sum of two Lorentzian lines with different widths (see Fig. 2, curve 5). However, many highly conducting polyaniline films are almost amorphous and corresponding ESR lines are single Lorentzian lines. Earlier,²¹ we assumed that the conductivity of polyaniline is controlled by the conductivity of the domains between amorphous (quasi-1D) domains rather than by the amorphous domains themselves. We believe that the interrelation between the ESR lineshape and the conductivity deserves additional investigation.

Effect of oxygen on the ESR linewidth of films and powders. It is known that in the presence of molecular oxygen the ESR lines of polyaniline and other conducting polymers can be broadened. The key features of the effect of O_2 on the ESR linewidths of conducting polymers were explained by a model³⁰ which implies that the paramagnetic O_2 molecule adds to the polymer and the exchange interaction between spins of the immobilized oxygen and mobile electron causes line broadening when the species approach one another. This broadening depends on both the amount of dioxygen added and the electron mobilities.

Oxygen causes no broadening of the ESR line of the films containing no CSA (see Table 3). This can be explained by the fact that O_2 does not add to isolated chains; efficient dioxygen addition is only possible by inserting between neighboring chains. This assumption is substantiated by the data on the effect of oxygen on the PAN1

and PAN2 powders.²⁴ Oxygen causes a much more efficient broadening of the PAN1 line, which is consistent with the shorter chain-chain distance in PAN1 (see Table 2).

According to the data listed in Table 3, the oxygen-induced broadening of the ESR line of the films considered as function of the linewidth in vacuum passes through a maximum (for the films prepared from fresh paste). Since the linewidth in vacuum increases with the chain-chain distance, one can conclude that oxygen poorly adds to both highly close-packed chains (owing to steric hindrances) and to isolated chains (due to weak interaction).

Role of anisotropy of the *g*-factor. The 2-mm ESR spectra of the PAN1 and PAN2 powders in air were reported.²¹ The ESR spectrum of PAN2 exhibits anisotropy of the *g*-factor ($g_{xx} = 2.0014$, $g_{yy} = 2.00275$, $g_{zz} = 2.00305$) while that of PAN1 is a line. This is naturally explained by the fact that in PAN1 the exchange interaction is stronger than in PAN2; therefore, anisotropy of the *g*-factor for PAN1 is averaged by the exchange interaction.

The second moment of the ESR line simulated with the *g*-factors listed above is $7 \cdot 10^{-3}$ for the 3-cm and 1.6 mT² for the 2-mm ESR band. Thus, anisotropy of the *g*-factor makes a negligible contribution to the second moment in the 3-cm band. The taking into account of anisotropy of the *g*-factor makes it possible to explain the broadening of the ESR line of the PAN1 powder from 0.11 to 0.31 mT on going from the 3-cm band to the 2-mm band. This line broadening is consistent with an increase in the \bar{H}_z^2 parameter from 0.6 mT to $0.6 + 1.6 = 2.2$ mT provided that the AT^2 term in relation (6) is small.

Thus, *m*-cresol can dope polyaniline without CSA additives, but the conductivity of the films containing no CSA is ten orders of magnitude lower than that of the films containing CSA additives. The data obtained in this work show that this can be explained by the weak interaction between polyaniline chains without CSA; CSA behaves as a "glue" and thus causes the exchange interaction between electron spins of neighboring chains to strengthen, which leads to higher conductivity, narrowing of the ESR lines, decrease in the number of localized electrons, and is responsible for the Lorentzian shape of the ESR line.

We proposed a relation, which describes the temperature dependence of the ESR linewidth for polyaniline. The linewidth is represented by the sum of two terms. One of them is due to the spin-phonon interaction and increases in proportion to T^2 as the temperature increases. The second term in the 3-cm range is due to the HFI between electrons and nuclei and decreases with an increase in temperature owing to the motion of electrons along polymer chains and the exchange interaction between electrons of neighboring chains. The exchange interaction has no effect on the first term. From comparison of the experimental and theoretical temperature de-

pendences of the ESR linewidth we determined the interchain distance and some other parameters.

Differences in the interchain distances make it possible to explain not only different film conductivities but also different degrees of ESR line broadening by O₂ and distinctions between the published 2-mm ESR spectra of polyaniline.

It was found that in the presence of CSA the conductivity and the ESR spectra of the films depend on the prehistory of the solution from which the films were cast and change with time. These changes occur faster as temperature increases, which can be explained by changes in the interchain distances. In contrast to optical spectra, the ESR spectra are rather sensitive to these changes and allow one to monitor the aggregation of chains. This may appear to be useful in studies of routes to enhanced conductivity of polyaniline and other conducting polymer films.

This work was financially supported by the Russian Foundation for Basic Research (Project No. 03-03-32251-a).

References

1. Y. Cao, P. Smith, and A. J. Heeger, *Synth. Met.*, 1992, **48**, 91.
2. J. K. Avlyanov, Y. Min, A. G. MacDiarmid, and A. J. Epstein, *Synth. Met.*, 1995, **72**, 65.
3. A. G. MacDiarmid and A. J. Epstein, *Synth. Met.*, 1995, **69**, 85.
4. Y. Xia, J. M. Wiesinger, A. G. MacDiarmid, and A. J. Epstein, *Chem. Mater.*, 1995, **7**, 443.
5. A. G. MacDiarmid, *Synth. Met.*, 1997, **84**, 27.
6. L. Dai, J. Lu, B. Matthews, and A. W. H. Mau, *J. Phys. Chem. B*, 1998, **102**, 4049.
7. R. S. Kolman and A. J. Epstein, in *Handbook of Conducting Polymers*, Eds T. A. Skotheim, R. L. Eisenbaumer, and J. R. Reynolds, Marcel Dekker, New York, 1998, p. 85.
8. O. T. Ikkala, L.-O. Pietilä, P. Passiniemi, T. Vikki, H. Österholm, L. Ahjopalo, and J.-E. Österholm, *Synth. Met.*, 1977, **84**, 55.
9. Z. H. Wang, A. Ray, A. G. MacDiarmid, and A. J. Epstein, *Phys. Rev. B*, 1991, **43**, 4373.
10. Z. H. Wang, E. M. Scherr, A. G. MacDiarmid, and A. J. Epstein, *Phys. Rev. B*, 1992, **45**, 4190.
11. A. Raghunathan, P. K. Kahol, and B. J. McCormick, *Synth. Met.*, 1999, **100**, 205.
12. A. Abragam, *The Principles of Nuclear Magnetism*, Clarendon Press, Oxford, 1961, Ch. 9 and 10.
13. P. K. Kahol and M. Mering, *Synth. Met.*, 1986, **16**, 257.
14. K. R. Brenneman, J. Feng, Y. Zhou, A. G. MacDiarmid, P. K. Kahol, and A. J. Epstein, *Synth. Met.*, 1999, **101**, 785.
15. K. Mizoguchi, N. Kachi, H. Sakamoto, K. Kume, K. Yoshioka, S. Masubuchi, and S. Kazama, *Synth. Met.*, 1997, **84**, 695.
16. K. Kanemoto, J. Yamauchi, and A. Adachi, *Solid State Commun.*, 1998, **107**, 203.
17. K. Kanemoto and J. Yamauchi, *Synth. Met.*, 2000, **114**, 79.
18. C. P. Slichter, *Principles of Magnetic Resonance*, Ed. P. Fulde, Springer-Verlag, Berlin—Heidelberg—New York, 1980, Ch. 5.
19. C. D. Jeffries, *Dynamic Nuclear Orientation*, Interscience Publishers, New York—London—Sydney, 1963, Ch. 3.
20. V. I. Krinichnyi, H.-K. Roth, G. Hinrichsen, F. Lux, and K. Lüders, *Phys. Rev. B*, 2002, **65**, 155205.
21. A. V. Kulikov, V. R. Bogatyrenko, O. V. Belonogova, L. S. Fokeeva, A. V. Lebedev, T. A. Echmaeva, and I. G. Shunina, *Izv. Akad. Nauk, Ser. Khim.*, 2002, 2057 [*Russ. Chem. Bull., Int. Ed.*, 2002, **51**, 2216].
22. C. J. Magon, R. R. de Souza, A. J. Costa-Filho, E. A. Vidoto, R. M. Faria, and O. R. Nascimento, *J. Chem. Phys.*, 2000, **112**, 2958.
23. G. I. Likhtenshtein, A. I. Kotelnikov, and A. V. Kulikov, *Dokl. Akad. Nauk SSSR*, 1981, **257**, 733 [*Dokl. Chem.*, 1981 (Engl. Transl.)].
24. A. V. Kulikov, V. R. Bogatyrenko, O. V. Belonogova, and L. S. Fokeeva, *Izv. Akad. Nauk, Ser. Khim.*, 2000, 1762 [*Russ. Chem. Bull., Int. Ed.*, 2000, **49**, 1742].
25. M. E. Jozefowics, R. Laversanne, H. H. S. Javadi, A. J. Epstein, J. P. Pouget, X. Tang, and A. G. MacDiarmid, *Phys. Rev. B*, 1989, **39**, 12959.
26. B. Beau, J. P. Travers, and E. Banka, *Synth. Met.*, 1999, **101**, 772.
27. F. D. Dyson, *Phys. Rev.*, 1955, **98**, 349.
28. C. P. Poole, *Electron Spin Resonance. Comprehensive Treatise on Experimental Techniques*, Interscience Publishers, A Division of J. Wiley and Sons, New York—London—Sydney, 1967.
29. D. Berner, J. Davenas, D. Djurado, M. Nechtschein, P. Rannou, and J.-P. Travers, *Synth. Met.*, 1999, **101**, 727.
30. E. Houze and M. Nechtschein, *Phys. Rev. B*, 1996, **53**, 14309.

Received February 10, 2005;
in revised form August 15, 2005